MULTITEMPORAL FUZZY MARKOV CHAIN-BASED CLASSIFICATION OF VERY HIGH RESOLUTION IMAGES OF AN URBAN SITE

G. A. O. P. Costa [a, *], R. Q. Feitosa [a], L. F. G. Rego [b]

[a] Department of Electrical Engineering
[b] Department of Geography
Pontifícia Universidade Católica do Rio de Janeiro Rua Marquês de São Vicente 225, Gávea, Rio de Janeiro, CEP: 22453-900, RJ, Brasil – (gilson, raul)@ele.puc-rio.br, regoluiz@puc-rio.br

KEY WORDS: Multitemporal, Interpretation, Fuzzy Logic, High Resolution, Urban, Land Use, Land Cover

ABSTRACT:

This work discusses the application of the cascade, multitemporal classification method based on fuzzy Markov chains originally introduced in (Feitosa et al. 2009), over a set of IKONOS images of urban areas within the city of Rio de Janeiro, Brazil. The method combines the fuzzy, monotemporal, classification of a geographical region in two points in time to provide a single unified result. The method does not require knowledge of the true class at the earlier date, but uses instead the attributes of the image object being classified at both the later and the earlier date. A transformation law based on class transition possibilities projects the earlier classification to the later date before combining both results. While in (Feitosa et al. 2009) the fuzzy Markov chain-based method was evaluated over a series of medium resolution, LANDSAT images, in this work very high resolution images were processed. Additionally, while the target area of the previous work was characterized predominantly by agricultural use, in this work an urban area was the subject of classification. The results showed that the performance of the multitemporal method was consistently superior to that of the monotemporal classification of the study area, and confirmed the robustness of the fuzzy Markov chain-based method with respect to sensor characteristics and target sites.

1. INTRODUCTION

Sequences of Remote Sensing images of the same geographical area acquired at different points represent a valuable source of information that can be used to improve the accuracy and reliability of classification-based image analysis.

Most traditional multidate image classification methods can be regarded as "post-classification" approaches (Weismiller et al., 1977), which are decisively dependent on the accuracy of the initial classifications. More powerful alternatives, called "cascade-classification" approaches (Swain, 1978) use all the information contained in the image sequence, trying to explore the correlation contained in the temporal data sets.

Feitosa et al. (2009) presented a detailed overview of the most relevant efforts towards automatic cascade multitemporal schemes found in the literature. These attempts include probabilistic methods, methods based on neural networks and multi-classifier approaches.

A first attempt towards a fuzzy cascade classification technique can be found in (Mota et al., 2007). That method is restricted to applications where the true class of the object being classified at an earlier time is known. Feitosa et al. (2009) described a new fuzzy cascade multitemporal classification model, explicitly based on fuzzy Markov chains, in which object features other than the true classification are used as the information from the earlier date. In the later method, before the classifications of two images at two dates are combined, the fuzzy classification at the earlier date undergoes a temporal transformation that projects it onto the later date.

This work discusses the application of the cascade, multitemporal classification method introduced in (Feitosa et al. 2009), originally applied over an agricultural over a set of IKONOS II images of urban areas within the city of Rio de Janeiro, Brazil.

2. FUZZY MARKOV CHAINS

This section describes briefly the concept of Fuzzy Markov Chain (FMC). A complete and more general presentation about this technique and the related concepts may be found in (Avrachenkov and Sanchez, 2002).

In this work we consider images acquired at dates $t_0+t\Delta t$, where t_0 is some stipulated initial time, Δt is a given time interval, and t is any integer number. For simplicity the date $t_0+t\Delta t$ will be denoted from this point on as time t, and $t_0+(t+1)\Delta t$ as time $t+1$, for $t \in Z$.

Let $\mathbf{\Omega} = \{\omega_1, \omega_2, \ldots, \omega_n\}$ be a set of n distinguishable land-use/land-cover (LULC). A binary fuzzy relation can be defined on the Cartesian product $\mathbf{\Omega}\times\mathbf{\Omega}$ represented by a $n\times n$ transition matrix $\mathbf{T} = \{\tau_{ij}\}$. The symbol τ_{ij} stands for the possibility that an image object belongs to the class $\omega_i \in \mathbf{\Omega}$ at time t and to the class $\omega_j \in \mathbf{\Omega}$ at time $t+1$, with $0 \le \tau_{ij} \le 1$, for $i,j = 1,\ldots,n$.

This can be pictorially described by a class transition diagram (Figure 1), a weighted directed graph whose nodes correspond to classes and links to plausible class transitions between t and $t+1$. Each link is labeled with the class transition possibility τ_{ij}. For simplicity links with $\tau_{ij} = 0$ are not drawn.

* Corresponding author.

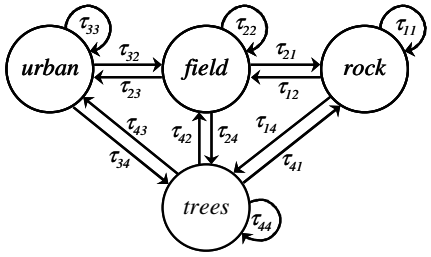

Figure 1. Class transition diagram with four classes.

The vector ${}^{t}\boldsymbol{\alpha} = [{}^{t}\alpha_1,\ldots,{}^{t}\alpha_n]$ with $0 \le {}^{t}\alpha_i \le 1$ represents, for a particular image object, the fuzzy classification defined over $\boldsymbol{\Omega}$ at time *t,* where ${}^{t}\alpha_i$ denotes the membership value of the object to class ω_i (for all $\omega_i \in \boldsymbol{\Omega}$) at time *t.* It is further assumed that ${}^{t}\alpha_i$ is a function of attribute values of the image object at time *t.*

Based on the fuzzy label vector ${}^{t}\boldsymbol{\alpha}$ and on the transition matrix **T**, the Fuzzy Markov Chain Model estimates the class membership values, represented by the vector ${}^{t+1}\boldsymbol{\beta} = [{}^{t+1}\beta_1,\ldots,{}^{t+1}\beta_n]$ for the same object one time unit later by applying the following formula:

$$ {}^{t+1}\beta_j = \underset{i=1,\ldots,n}{\perp} \left\{ \top\left({}^{t}\alpha_i, \tau_{ij} \right) \right\} \tag{1} $$

for $i,j = 1,\ldots,n$. The symbols $\top$ and $\perp$ represent respectively a *t-norm* and a *s-norm*.

The transition law introduced in Equation (1) can be expressed in a more compact form by the equation below.

$$ {}^{t+1}\boldsymbol{\beta} = {}^{t}\boldsymbol{\alpha} \circ \mathbf{T} \tag{2} $$

In the expression "$\mathbf{A}\circ\mathbf{B}$", the symbol "$\circ$" denotes a special type of matrix multiplication, analogous to conventional matrix multiplication, where the product is replaced by a *t-norm* and the summation is replaced by a *s-norm* operator.

The symbols ${}^{t+1}\boldsymbol{\beta}$ and ${}^{t+1}\boldsymbol{\alpha}$ denote different distributions although both refer to the same object at the date *t+1*. While ${}^{t+1}\boldsymbol{\alpha}$ has been computed based on feature values at time *t+1* without any temporal transition transformation, ${}^{t+1}\boldsymbol{\beta}$ is the result of applying the FMC transition law, Equation (2), upon the membership grades in ${}^{t}\boldsymbol{\alpha}$ computed on the feature values of the image object corresponding to the same geographical object at time *t.*

3. MULTITEMPORAL CLASSIFICATION MODEL

3.1 Problem statement

Let ${}^{t}\mathbf{I}$ and ${}^{t+1}\mathbf{I}$ denote two co-registered images of the same geographical area acquired respectively at dates *t* and *t+1*. Accordingly, ${}^{t}\mathbf{x}$ and ${}^{t+1}\mathbf{x}$ stand for the feature vectors composed of spectral and spatial feature values describing the same geographical object respectively in ${}^{t}\mathbf{I}$ and ${}^{t+1}\mathbf{I}$. We further denote with ${}^{t}\mathbf{w}$ and ${}^{t+1}\mathbf{w}$ the *crisp* label vectors for the object being analyzed at times *t* and *t+1*. Both ${}^{t}\mathbf{w}$ and ${}^{t+1}\mathbf{w}$ are *n*-dimensional unitary vectors of the form [0 … 1 … 0] having "1" in its *i*-th component and "0" otherwise, indicating that the object belongs to the class ω_i at a particular time. Formally, ${}^{t}\mathbf{w}$ and ${}^{t+1}\mathbf{w}$ belong to a *n* dimensional space $\boldsymbol{\Omega}^n$, where:

$$ \boldsymbol{\Omega}^n = \{\, \mathbf{w} = [\, w_1,\ldots,w_n] \mid w_i \in \{0,1\} \text{ for all } i = 1,\ldots,n \text{ and } \|\mathbf{w}\| = 1 \,\} \tag{3} $$

The multitemporal classification problem treated in the present work consists of identifying the vector ${}^{t+1}\mathbf{w}$ for each image object, based on the feature vectors ${}^{t}\mathbf{x}$ and ${}^{t+1}\mathbf{x}$, in other words, it is about finding a function **M** of the form:

$$ {}^{t+1}\mathbf{w} = \mathbf{M}\,({}^{t}\mathbf{x}, {}^{t+1}\mathbf{x}) \tag{4} $$

3.2 General classification model

The terms monotemporal and multitemporal will be used hereafter to designate classifiers whose inputs refer respectively to a single date or to multiple dates.

The outcome of the multitemporal classifier can be viewed as the fusion of the outcome of two monotemporal classifiers. Let the first monotemporal classifier be represented by a function ${}^{L}\mathbf{C}$ that computes membership values for the object being classified at the later time *t+1* based exclusively on the feature values at time *t+1*, extracted from image ${}^{t+1}\mathbf{I}$. The monotemporal classifier ${}^{L}\mathbf{C}$ produces a *n*-dimensional *fuzzy* label vector denoted by ${}^{t+1}\boldsymbol{\alpha} = [{}^{t+1}\alpha_1, {}^{t+1}\alpha_2,\ldots,{}^{t+1}\alpha_n]$, where ${}^{t+1}\alpha_i$ stands for the membership of the image object assigned by ${}^{L}\mathbf{C}$ to the class ω_i, for all $\omega_i \in \boldsymbol{\Omega}$ and for at least one *i*, ${}^{t+1}\alpha_i \neq 0$. So, ${}^{L}\mathbf{C}$ can be viewed as a function of the form:

$$ {}^{t+1}\boldsymbol{\alpha} = {}^{L}\mathbf{C}\,({}^{t+1}\mathbf{x}) \tag{5} $$

A second *monotemporal* ${}^{E}\mathbf{C}$ is applied to the object feature vector ${}^{t}\mathbf{x}$ at time *t*. Analogously to the first monotemporal classifier, it generates a fuzzy label vector ${}^{t}\boldsymbol{\alpha}$, formally:

$$ {}^{t}\boldsymbol{\alpha} = {}^{E}\mathbf{C}\,({}^{t}\mathbf{x}) \tag{6} $$

Since ${}^{t}\boldsymbol{\alpha}$ refers to the membership distribution at the earlier time *t* and our interest is in the classification at the later time *t+1*, the FCM transition law is applied to infer the membership values at time *t+1* based on the membership values at *t.* Thus, if **T** is the class transitions matrix representing the class transitions in two consecutive instants, we may estimate the classification at time *t+1* by combining equations (2) and (6), yielding:

$$ {}^{t+1}\boldsymbol{\beta} = {}^{E}\mathbf{C}\,({}^{t}\mathbf{x}) \circ \mathbf{T} \tag{7} $$

The two fuzzy label vectors ${}^{t+1}\boldsymbol{\alpha}$ and ${}^{t+1}\boldsymbol{\beta}$ are then combined in the next step by an *aggregation* function **F** to form a *multitemporal* fuzzy label vector ${}^{t+1}\boldsymbol{\mu} = [{}^{t+1}\mu_1,\ldots,{}^{t+1}\mu_n]$ given by:

$$ {}^{t+1}\boldsymbol{\mu} = \mathbf{F}({}^{t+1}\boldsymbol{\alpha}, {}^{t+1}\boldsymbol{\beta}) = \mathbf{F}[{}^{L}\mathbf{C}\,({}^{t+1}\mathbf{x}), {}^{E}\mathbf{C}\,({}^{t}\mathbf{x}) \circ \mathbf{T}] \tag{8} $$

The final step is the defuzzification, performed by a function of the form:

$$ \mathbf{H}: [0,1]^n \rightarrow \Omega^n \tag{9} $$

that transforms the *fuzzy* label vector ${}^{t+1}\boldsymbol{\mu}$ into a *crisp* one. Putting it all together, the multitemporal classifier **M** is given by Equation (10).

$$ {}^{t+1}\mathbf{w} = \mathbf{M}({}^{t+1}\mathbf{x}, {}^{t}\mathbf{x}) = \mathbf{H}\{\, \mathbf{F}[{}^{L}\mathbf{C}\,({}^{t+1}\mathbf{x}), {}^{E}\mathbf{C}\,({}^{t}\mathbf{x}) \circ \mathbf{T}] \,\} \tag{10} $$

3.3 Particularization of the classification model

FMC models may be built using any *t-norm* and *s-norm* composition. We favor the *max-product* composition, since it leads to a simple multitemporal classification model with an intuitive interpretation,. Thus Equation (1) takes the form:

$$ {}^{t+1}\beta_j = \max_{i=1,\ldots,n} \{ {}^{t}\alpha_i \, \tau_{ij} \} \quad (11) $$

for $i,j = 1,\ldots,n$.

The defuzzyfication step is carried out by a hardening function **H** that selects the fuzzy set with the highest membership grade, formally:

$$ [w_1,\ldots,w_n] = \mathbf{w} = \mathbf{H}(\boldsymbol{\mu}) = \mathbf{H}([\mu_1,\ldots,\mu_n]), \text{ where } w_j = \begin{cases} 1 \text{ for } \mu_j = \max\{\mu_1,\ldots,\mu_n\} \\ 0 \text{ otherwise} \end{cases} \quad (12) $$

The aggregation function **F** is the product of corresponding elements of the input fuzzy vectors. Thus,

$$ {}^{t+1}\boldsymbol{\mu} = \mathbf{F}({}^{t+1}\boldsymbol{\alpha}, {}^{t+1}\boldsymbol{\beta}) = [{}^{t+1}\alpha_1 \, {}^{t+1}\beta_1, \ldots, {}^{t+k}\alpha_n \, {}^{t+1}\beta_n] \quad (13) $$

Putting it all together, the multitemporal classifier assigns the image object to the class $\omega_i \in \boldsymbol{\Omega}$ at time $t+1$, for which

$$ {}^{t+1}\mu_i = \max_k \left\{ {}^{t+1}\alpha_k \max_l \left({}^{t}\alpha_l \tau_{lk} \right) \right\} = \max_{k,l} \left\{ {}^{t}\alpha_l \tau_{lk} \, {}^{t+1}\alpha_k \right\} \quad (14) $$

holds.

3.4 Estimating transition possibilities

The estimation of transition possibilities basically selects the set of possibility values that maximizes the classification accuracy computed upon a given training set.

The estimation procedure consists of finding the set of transition possibility values $\mathbf{T}=\{\tau_{ij}\}$ that maximizes the selected accuracy function G, for the selected image objects S of image objects at the later date (the training set) and for the selected monotemporal classifiers. This is formally expressed by:

$$ \mathbf{T} = \arg\max_{\tilde{\mathbf{T}}} \left\{ G\left(S, {}^{E}\mathbf{C}, {}^{L}\mathbf{C}, \tilde{\mathbf{T}}\right) \right\} \quad (15) $$

The computation of transition possibilities defined in Equation (17) involves an optimization procedure. The classification model introduced in the previous sections is actually not bound to any particular parameter optimization technique. In this work, the average class accuracy was used as accuracy function, and a Genetic Algorithm was the optimization technique used to estimate transition possibilities (Schmiedle et al., 2002).

4. EXPERIMENTS

The experiments described in the following sections were designed to evaluate the proposed method over a set of high resolution IKONOS II images. The experiments aimed at comparing the outcome of the multitemporal classification with that of the monotemporal classification of the later image. We also investigated the performance of the method tuning the performance of the earlier monotemporal classifier, as described in Section 4.4. The idea was to investigate how the method behaves with different (increasing) performances of the earlier monotemporal classifier.

The data set used in all experiments is described in the next section. Afterward, the design of the particular monotemporal classifier that composes the multitemporal scheme in the experiments is presented. The following two sections describe respectively the monotemporal classifier design and the optimization technique used to estimate transition possibilities.

4.1 Description of the data set

The test site corresponds to a 14.4 km^2 area, situated on the north face of the Tijuca National Park, within the city of Rio de Janeiro, an important Atlantic Forest reminiscent. The test-site is a subset of the area of interest of the PIMAR Project (Remote Environmental Monitoring Program), which aims at monitoring the suppression of rainforest on conservation units inside the municipality of Rio de Janeiro through high resolution optical remote sensing images (PIMAR, 2010).

This area was selected as test-site because of the noticeable sprawl of informal dwellings over legally protected natural areas. Moreover, the area contents various instances of all land cover classes considered by the PIMAR Project.

Two pan-shaped, orthorectified IKONOS II images were used in the experiments. The images actually take part of two stereo pairs, each pair acquired on the same orbit, with different elevation angles. The orthorectification was performed using digital elevation models derived from each stereo pair. For each year the image with the highest elevation angle was chosen and submitted to orthorectification.

It is important to note that because of the time of the year the images were acquired – March 2008 (late summer) and June 2009 (late autumn) respectively –, they present quite different illumination conditions, with an important presence of clouds in the 2009 image. No radiometric correction or equalization was performed over the orthorectfied images.

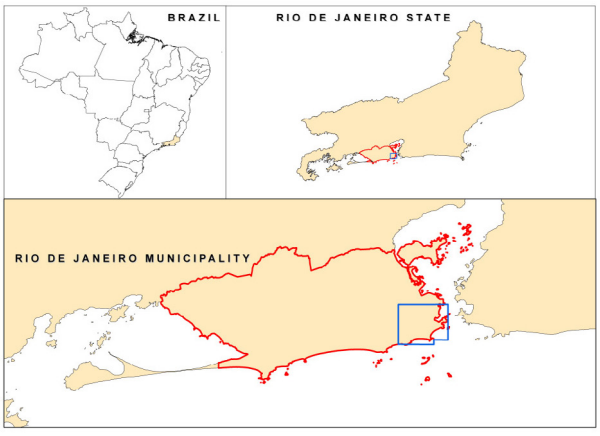

Figure 2. Area of the test-site in Rio de Janeiro municipality.

The orthorectified IKONOS II images were segmented using the multiresolution segmentation algorithm proposed by Baaz and Shäpe (2000), through the Definiens Developer 7 software. The parameters chosen for the segmentation procedure were

such that the resulting segments were small in size, as defined by the low scale parameter value, giving priority to color homogeneity instead of coherently shaped segments. The idea was to absolutely avoid that the segments disrespect the border between two different land cover objects.

Parameter	Value
Scale	30
Color	0.9
Shape	0.1
Compactness	0.5
Smoothness	0.5
Layer weights (bands 1, 2, 3 and 4)	1,1,1,1

Table 1. Segmentation parameters used in the experiments.

All segments generated from the two images were duly, visually classified by specialists. Table 2 describes the land-use classes considered. Actually, shadow segments were also classified as such, but they were not considered in the experiments.

After classification, all segments from each class in 2008 were merged to the adjacent segments of the same class, generating larger area segments. Then, only the segments from 2009 that fell completely inside the large 2008 segments (generated from the merging procedure) were selected.

For those selected segments (generated through the segmentation of the 2009 image), feature attributes were calculated from each of the two images. The feature extraction procedure was also implemented on the Definiens Developer software. The features extracted for each segment were: mean values of the four spectral bands and the textural entropy feature (for all bands in all directions).

The basic idea of the procedure described above was to produce a set of segments with class labels for 2008 and 2009, and with two sets of attributes, extracted respectively from the 2008 and 2009 images. Table 3 shows the number of segments assigned to each class, in each year and the class transitions observed from 2008 to 2009.

Label	Class	Description
Rock (ω_1)	Rock	Exposed rock (granite) formations.
Field (ω_2)	Grass field	Grass fields naturally formed over thin soil or created by anthropogenic activities.
Urban (ω_3)	Urban Area	Constructed area (buildings, roads, etc.) including bare soil areas
Trees (ω_4)	Arboreous Vegetation	Individual or clusters of trees (inside urban areas or not).

Table 2. LULC classes considered in the esperiments.

	2009				
2008	Rock	Field	Urban	Trees	Total
Rock	188	10	0	1	199
Field	11	421	66	153	651
Urban	0	9	5594	220	5823
Trees	1	194	390	33947	34532
Total	200	634	6050	34321	41205

Table 3. Class transitions from 2008 to 2009.

4.2 Monotemporal classifier design

A simple design is adopted in our experiments for the earlier ($^{t}\mathbf{C}$) and later ($^{t+1}\mathbf{C}$) monotemporal image classifiers. Feature vectors $\mathbf{x}$ are built for each segment by stacking the attribute value of the segments (recorded at a specific date). It is assumed that all classes ω_i can be appropriately modelled by a Gaussian-shaped membership function $\mathbf{MF}_{\omega i}(\mathbf{x})$ given by the formula below:

$$MF_{\omega i}(\mathbf{x}) = \exp\left[-\frac{\left(\mathbf{x}-\bar{\mathbf{x}}_{\omega i}\right)^{T}\sum_{\omega i}^{-1}\left(\mathbf{x}-\bar{\mathbf{x}}_{\omega i}\right)}{2}\right] \quad (16)$$

for $\omega_i \in \{rock, field, urban, trees\}$, where $\bar{\mathbf{x}}_{\omega i}$ and $\boldsymbol{\Sigma}_{\omega i}$ correspond respectively to the mean and to the covariance matrix of the class ω_i.

4.3 Optimization procedure

The transition possibility values were estimated, as mentioned in Section 3.4, by a Genetic Algorithm (GA) using as objective function the average class accuracy. The genes were the transition possibility values. The GA design used in the experiments was the same as in (Feitosa et al., 2009).

4.4 Simulating monotemporal classifiers with tunable performance

The multitemporal classification based on fuzzy Markov chains is evaluated for for monotemporal classifiers with varying performances. Such evaluation scheme can be done by defining a simulated monotemporal classifier $^{t+k}\mathbf{C}^*$ with tuneable performance, that is, for all image objects, we have:

$$^{t+k}\boldsymbol{\alpha}^* = m\ ^{t+k}\mathbf{W} + (1-m)\ ^{t+k}\boldsymbol{\alpha} \quad (17)$$

where $^{t+k}\mathbf{W}$ is the *true* crisp label vector, $^{t+k}\boldsymbol{\alpha}$ is the fuzzy label vector from the monotemporal classifier, and m is a *mixture factor* that takes values in the interval [0,1]. For $m = 0$, the simulated monotemporal classifier is identical to the monotemporal classifier described in the previous section; for $m = 1$, it is equal to the *ideal* classifier.

The monotemporal classifiers, $^{t+k}\mathbf{C}$, are replaced in our experiments by the simulated monotemporal classifier, $^{t+k}\mathbf{C}^*$, and a continuous variation of m permits to observe how the relative performance of the monotemporal classifiers affects the accuracy of the multitemporal model. It is worth anticipating at this point the low performance of the real monotemporal classifier described in Section 4.2 in comparison to state of the art classification approaches (see experiment results in the next section). This is convenient in view of the objective of the analysis since it permits to assess the multitemporal models for a wide range of monotemporal classification performances.

4.5 Results

The benchmark for the analysis reported in the subsequent sections is the outcome of the monotemporal classifiers that take part of the multitemporal scheme. As the object of comparison is the crisp classification of the later image segments, a defuzzification step was performed over the output of the fuzzy monotemporal classifier, simply assigning to each

segment the class for which it obtained the highest membership value.

In a sequence of experiments using the average class accuracy to estimate transition possibilities, the training set was built in the following way. The image objects were first separated in groups according to the class transition they undergone in two consecutive dates. To estimate the parameters of the monotemporal classifiers as well as the transition possibilities as described in previous sections, approximately 25% of the objects in each group are randomly selected to form the training set. The remaining 25% of the objects were used to evaluate the method in terms of average class accuracy at the later date.

Figure 2 shows the performance achieved by both the monotemporal and multitemporal. The points in the graph represent averages values computed over 30 executions of the same experiment, each time with a distinct random selection of training and testing objects. Each point is associated to a specific mixture factor *m*.

As it was expected, the average outcome of the monotemporal classifier for 2008 in the various experiments remain almost constant, varying from 75% to 76% (Figure 3). It is also noticeable that the classification performance of the monotemporal classifier for 2008 is considerably better that that of the monotemporal classifier for 2009, even when the mixture factor is equal to zero, even though the design of the earlier and later monotemporal classifiers are the same. That may be credited to the fact that there are a considerable amount of shadows in the 2009 image, basically due to the different solar elevation angles in the two images. Although the completely shaded areas (segments) were not considered in the experiments, the effect of the shadows on the segments that were not discarded may have influenced the capacity of the classifier to discriminate among the classes of interest. The human interpreted can, however, easily adapt to those conditions.

Anyhow, it is interesting to observe that the multitemporal classification method could benefit from the better monotemporal classification from 2009 (even when the mixture factor *m* is equal to zero) and improve the classification accuracy by approximately 6.6% (Figure 4) – from 76% to 81% (Figure 3).

As the performance of the earlier monotemporal classifier improves (for 2008), influenced by the increasing mixture factor, so does the performance of the multitemporal classifier for 2009, reaching an average class accuracy of over 89% – an improvement of approximately 16.9% (Figure 4).

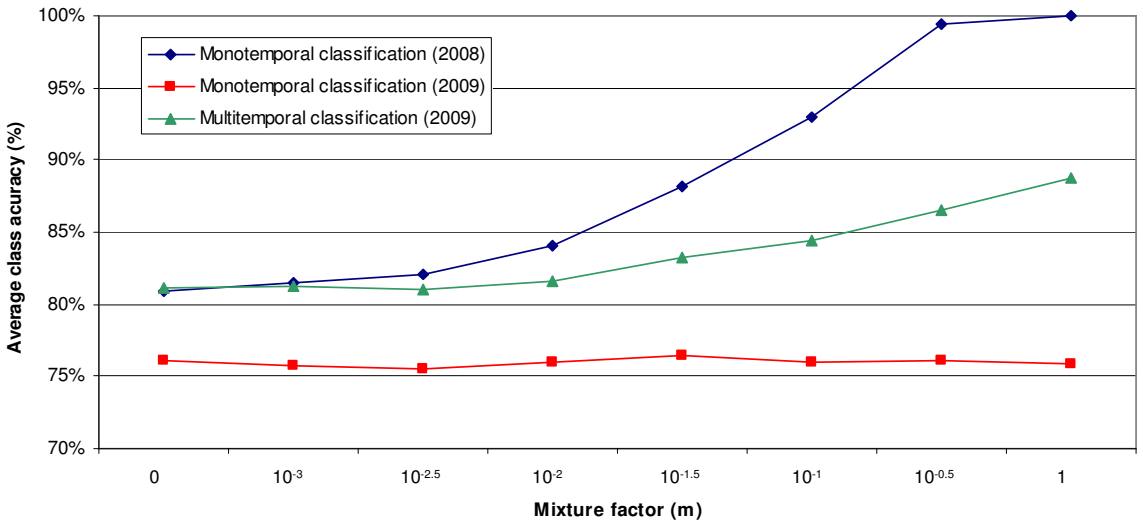

Figure 3. Performance of the monotemporal and multitemporal classifiers.

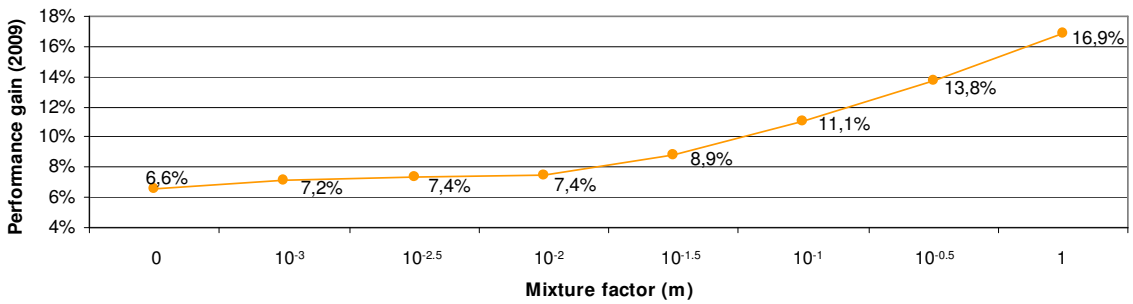

Figure 4. Performance gain in the classification of the 2009 image brought by the multitemporal classification.

5. CONCLUSION

In this paper, we applied the model proposed in (Feitosa et al., 2009) on a set of very high resolutionIKONOS II images of urban areas within the city of Rio de Janeiro, Brazil.

The results are consistent with the ones presented in (Feitosa et al., 2009), where series of Landsat images over an agricultural area were subjected to multitemporal interpretation.

The experiments results presented here and in (Feitosa et al., 2009) indicate that the multitemporal classification design based on fuzzy Markov chains generally brings an accuracy gain in relation to the monotemporal approach. Furthermore, it has been shown that the more accurate the information coming from the earlier date, the higher is its contribution to the multitemporal classification performance. In fact, the fuzzy Markov chain method seem to be particularly beneficial whenever there is information regarding the earlier date (t) that is significantly more accurate than the available information about the later date (t+1).

We should recall that the assumption underlying the proposed multitemporal classification model is the existence of a significant temporal correlation between the data sets. If an application does not meet this condition, the method is not expected to work properly at all.

Future research should tackle a number of other important issues. Experiments should be performed with more time points. In this case, conditions on the length of the Markov chain could also be investigated. Broader series of experiments with other geographic regions and types of images should also be carried out.

It would be also interesting to investigate other optimization algorithms, since genetic algorithms spend too much processing time and do not guarantee that the global optimum solution is found. A possible candidate for this optimization task could be some sort of least squares-based algorithm.

REFERENCES

Avranchenkov, K. E., Sanchez, E., 2002. Fuzzy Markov chains and decision-making. *Fuzzy Optimization and Decision Making* 1 (2), 143-159.

Baatz, M., Schäpe, A. 2000. Multiresolution segmentation – an optimization approach for high quality multi-scale image segmentation. In: Strobl, J., Blaschke, T. *Angewandte Geographische Informationsverarbeitung XII. Beiträge zum AGIT Symposium Salzburg 2000*, Herbert Wichmann Verlag, Karlsruhe.

Feitosa, R. Q., Costa, G. A. O. P., Mota, G. L. A., Feijó, B., 2009. Cascade classification of Multitemporal. *ISPRS International Journal on Photogrammetry and Remote Sensing* 64 (2), 159-170.

Mota, G. L. A., Feitosa, R. Q., Coutinho, H. L. C., Liedtke, C. E., Müller, S., Pakzad, K., Meirelles, M. S. P., 2007. Multitemporal fuzzy classification model based on class transition possibilities. *ISPRS International Journal of Photogrammetry and Remote Sensing* 62, 186-200.

PIMAR, 2010. Projeto PIMAR (Programa Integrado de Monitoria Remota de Fragmentos Florestais e de Crescimento Urbano no Rio de Janeiro). http://www.nima.puc-rio.br/sobre_nima/projetos/pimar (accessed 15 May 2010)

Schmiedle, F., Drechsler, N., Grosse, D., Drechsler, R., 2002. Heuristic learning based on genetic programming. Genetic *Programming and Evolvable Machines* 3 (4), 363-388.

Swain, P. H. 1978. Bayesian classification in a time-varying environment. *IEEE Trans. Sys. Man. and Cybern*. 12, 879-883.

Weismiller, R. A., Kristoof, S. J., Scholz, D. K., Anuta, P. E., Momen, S. A., 1977. Change detection in coastal zone environments. *Photogrammetric Engineering and Remote Sensing* 43, 1533-1539.

ACKNOWLEDGEMENTS

This work was supported by CNPq (Brazilian National Counsel of Technological and Scientific Development), FINEP (Brazilian Innovation Agency) and FAPERJ (Carlos Chagas Filho Research Support Agency of the State of Rio de Janeiro). We would also like to thank the Government of the State of Rio de Janeiro, Secretaria de Estado do Ambiente (SEA) for funding the PIMAR project.